MORPHOLOGY AND MECHANICAL PROPERTIES OF LOW-MOLECULAR -WEIGHT POLYETHYLENE AND ULTRAHIGH-MOLECULAR-WEIGHT POLYETHYLENE FILMS DRAWN UP TO 200-FOLD

Yuezhen Bin, Miwako Fukuda, Hiromichi Kurosu, and Masaru Matsuo*

Department of Textile and Apparel Science, Faculty of Human Life and Environment, Nara Women's University, Nara 630, Japan

SUMMARY: Ultrahigh-molecular-weight polyethylene (UHMWPE) and low-molecular-weight polyethylene (LMWPE) blend films were prepared by gelation/crystallization from solutions. UHMWPE with the viscosity-average molecular weight ($\overline{M}_v$) of 6×10^6 and three kinds of LMWPE with $\overline{M}_v < 5\times10^4$ were used. The LMWPE/ UHMWPE compositions chosen were 1/1, 2/1, 4/1 and 9/1. The resulting blend gels with the 9/1 composition (10% UHMWPE content) became films by evaporating the solvents, although LMWPE homopolymer gels have no ability to form films. The films with the above compositions could be readily elongated up to 200-fold in a hot oven. Such high elongation is assumed to be due to the existence of a suitable level of entanglements between UHMWPE and LMWPE chains. The orientational degree of LMWPE crystallites became poorer as the LMWPE content in the blend film increased, indicating a decrease in the number of entanglements. The storage modulus of the blend films at the same draw ratio decreased as the LMWPE content increased. The storage modulus of the 1/1 blend film with $\lambda = 200$ reached about 50 GPa at 20 °C but the storage modulus decreased drastically with further increase in the LMWPE content: the value of the 9/1 blend film with $\lambda = 200$ was less than 10 GPa. This means that a suitable level of entanglements between LMWPE and UHMWPE chains plays an important role in transmitting the drawing force effectively and promoting the orientational degree of the c-axis, owing to the crystal transformation from a folded to a fibrous type.

Introduction

The gel deformation has been well known as an ultra-drawing method to produce polyethylene fibers with high moduli and high strength.[1-4] The dry gel film has been produced by gelation/crystallization from dilute solutions using ultrahigh-molecular-weight polyethylene (UHMWPE) with molecular weight greater than 1×10^6. This procedure was proposed to solve the drawback that the attainable draw ratio of the melt-crystallized material decreases with increasing molecular weight and the samples with molecular weights $> 10^6$ cannot be drawn to ratios higher than 5-10. In our previous work,[5] it was found that for a sufficiently high molecular weight, the maximum achievable draw ratio principally depends on the concentration of the solution from which the gel was made. This phenomenon was attributed to a reduced number of entanglements per molecule in solution-cast or solution-spun polymers in comparison with those obtained from the melt. Matsuo et al. determined the critical concentration by the measurement of solution viscosity since it is basically related to the size or extension in space of the macromolecules.[6] The viscosity-concentration data indicated that there exists an apparent critical concentration range where there is an abrupt change in the concentration dependence of the viscosity. This critical concentration is

 CCC 1022-1360/99/$ 17.50+.50/0

assumed to correspond to the onset of overlap of the randomly coiled molecules in solutions. Films produced by gelation/crystallization from solution (critical concentration 0.4 g/100 ml) could be readily elongated to a draw ratio of λ = 300. For such ultra-drawn films, the maximum Young's modulus reached 215 GPa and tensile strength 6 GPa.[7] In the undeformed state, the gel of UHMWPE could form a film composed of rod-like textures oriented parallel to the plane of the dry gel film. Within the rod, large-crystal lamellae like single-crystal mats were highly oriented with their flat faces parallel to the rod surface.[8,9]

In contrast, the gels of low-molecular-weight polyethylene (LMWPE) (viscosity-average molecular weight less than 3×10^5) were found to have no ability to form a film on drying; instead, they broke up into flakes.[10] They were composed of two-dimensional spherulites stacked on top of one another to form periodic structures parallel to the plane of the dry gel. This indicates that there should be no entanglement in the crystal mats because the surface of the crystal would contain only regular folded chain loops. To analyze this problem, the crystallinities of dry gels of LMWPE were measured. The values for LMWPE gels with $\overline{M}_v >$ 80 000 were above 80 %. These values were almost equal to the values of UHMWPE and were higher than those of LMWPE melt films. This was attributed to the relatively short chain length available for the formation of the amorphous phase per molecule; as a result, there was an insufficient level of chain entanglements to form films.

However, LMWPE can produce fibers with Young's modulus of about 70 GPa by a particular melt spinning.[11] The X-ray results from undrawn and drawn fibers indicated that the preferential orientation of the c-axis is due to the crystal transformation from a folded to fibrous type. Such fibers have advantage as high-modulus and high-strength fibers in industrial fields since the production rate of high-modulus fibers from UHMWPE gels is far below commercially interesting speeds. Actually, the drawability of melt films prepared from UHMWPE is lower than that of melt films prepared from LMWPE because of a number of entanglements. Even so, Young's modulus higher than 100 GPa has never been reported for LMWPE fibers and films.

This paper deals with ultra-drawing of blend gel films of UHMWPE and LMWPE for the purpose of preparing high-modulus (> 100 GPa) and high-strength fibers with commercially interesting speeds since the viscosity of solution undergoes a drastic decrease with increasing content of LMWPE. However, detailed information concerning UHMWPE and LMWPE blends prepared by gelation/crystallization from semidilute solutions has never been reported. Our attention is concentrated on the two interesting problems. One is the film formation of the gel, and the other is the greatest significant drawability of the film. Surprisingly, the blends with 90% LMWPE could be elongated up to a 200-fold. The possibility of drawing successfully up to 200-fold becomes slightly lower as the LMWPE content increases. The morphology and mechanical properties of dry gel films as a function of the LMWPE content are investigated using wide-angle X-ray diffraction (WAXD), small-angle X-ray scattering (SAXS), differential scanning calorimetry, small-angle light scattering (SALS) and complex dynamic tensile modulus.

Experimental

The samples used in the experiments were UHMWPE (Hercules 1900/90189) with a viscosity-average molecular weight ($\overline{M}_v$) of 6×10^6 and three kinds of LMWPE, Sumikathen G201, G806, G808 whose $\overline{M}_v$ are 4.13×10^4, 1.95×10^3 and 1.53×10^3, respectively. The degree of branching of the three kinds of LMWPE is about 2.5 CH_3/100 C. The solvent was decalin. The LMWPE-UHMWPE compositions chosen were 1/1, 2/1, 4/1 and 9/1. Decalin solutions were prepared by heating the well-blended polymer-solvent mixture at 135 °C for 40 min under nitrogen. The concentration of UHMWPE was fixed being 0.4 g/100 ml. The solutions were stabilized with 3% w/w of an antioxidant (2,6-di-*tert*-butyl-4-methylphenol) relative to

PE. The hot homogenized solution was quenched to room temperature by pouring into an aluminum tray, thus generating a gel. Decalin was allowed to evaporate from the gel under ambient conditions. Surprisingly, even the dry gels with 9/1 composition could form a film. The resulting dry gel film was vacuum-dried for 1 day to remove residual traces of decalin.

The dry gel film was cut into strips of 30 mm length and 10 mm width. The specimens were placed in an oven at 135 °C for 5 min and elongated manually up to the desired ratio. Immediately after stretching, the stretcher with the sample was quenched to room temperature. The draw ratio was determined in a usual way by measuring the displacement of ink marks placed 1 mm apart on the specimen prior to drawing.

The density of the films was measured by pycnometry with chlorobenzene-toluene. Since the density was very dependent on the presence of residual solvent in the film, great care was taken to remove the solvent. Samples were cut into fragments and subsequently vacuum-dried for 1 day prior to measuring the density. Crystallinity was calculated assuming intrinsic densities of crystalline and amorphous phases to be 1.000 and 0.852 g cm^{-3}, respectively.[12)]

The complex dynamic tensile modulus was measured at 10 Hz over the temperature range from - 150 to 170 °C by using a viscoelastic spectrometer (VES-F) obtained from Iwamoto Machine Co. Ltd. The length of the specimen between the jaws was 40 mm and the width about 1.5 mm. During measurements, the film was subjected to a static tensile strain in order to place the sample in tension during the axial sinusoidal oscillation, which had a peak deformation of 0.05 ~ 0.1%. The complex dynamic modulus was measured by imposing a small dynamic strain to assure linear viscoelastic behavior of the specimens.[13)]

Measurements of melting point, birefringence, wide-angle X-ray diffraction, small-angle X-ray diffraction and small-angle light scattering are described in detail elsewhere.[14)]

Results and Discussion

Figure 1 shows WAXD patterns (end view) for 1/1 and 9/1 blends observed for three kinds of LMWPE, G201, G806, and G808, and UHMWPE. The WAXD patterns indicate the preferential orientation of the c-axis perpendicular to the film surface. Profiles of the WAXD patterns are hardly affected by the composition but the orientational degree becomes duller with decreasing molecular weight of LMWPE.

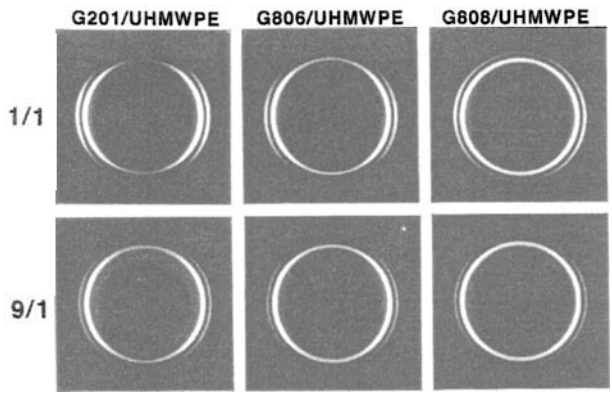

Fig. 1 WAXD and SAXS patterns (end view) for the 1/1 and 9/1 blends of three kinds of LMWPE, G201, G806, and G808, and UHMWPE

Figure 2 shows SAXS patterns (end view) for the undrawn LMWPE(G808)-UHMWPE blend films with 1/1, 2/1, 4/1 and 9/1 compositions. The SAXS patterns show the meridional scattering having a maximum corresponding to a long period of 10 - 11 nm and scattering arcs becoming longer with increasing LMWPE content. This indicates that the dried gel films are composed of highly oriented crystal lamellae with their flat faces parallel to the film surface. The WAXD and SAXS patterns together indicate that in the lamellar crystals constituting the gel, the c-axes are oriented perpendicular to the large flat faces.

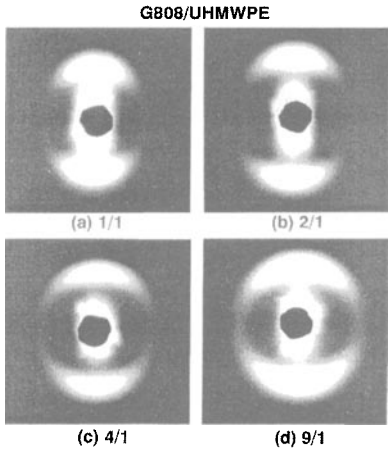

Fig. 2
SAXS patterns (end view) for the undrawn LMWPE(G808)-UHMWPE blend films with 1/1, 2/1, 4/1, and 9/1 compositions

In order to obtain more detailed information, SAXS intensity distributions were observed by the PSPC system for the undrawn blends and the UHMWPE homopolymer film in the meridional direction. Figures 3a,b,c show the results for G201, G806 and G808, respectively, in which the composition 0/1 means the UHMWPE dry gel film prepared from 0.4 g/100 ml.

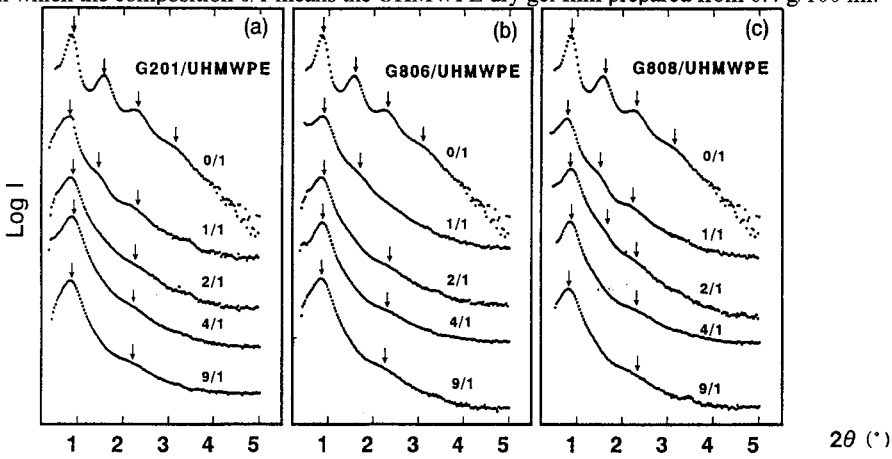

Fig. 3 SAXS intensity distributions for the undrawn blends and the UHMWPE homopolymer in the meridional direction by the PSPC system: (a) G201, (b) G806, (c) G808

The profiles at each LMWPE/UHMWPE composition are almost equal in spite of the adoption of three kinds of LMWPE with different molecular weights. The profiles of the scattered intensity distribution show that the scattering maxima become more indistinct as the LMWPE content increases. This result is in good agreement with the previous results[15] that

the scattered maxima observed on the LMWPE(G201)-UHMWPE gel films became more indistinct as the LMWPE (G201) content increased. This result presumably indicates that LMWPE has no ability to form large lamellae which can become highly oriented with their large flat faces parallel to the film surface, when the gels are dried by slow evaporation of the solvent.

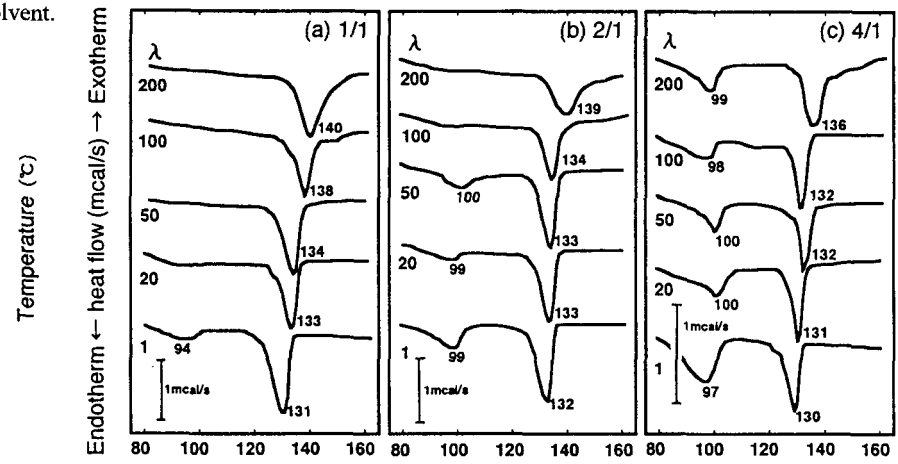

Fig. 4 DSC curves as a function of the draw ratio measured for the 1/1, 2/1 and 4/1 blend films of LMWPE(G808)-UHMWPE

Figures 4 show the change in the profile of the DSC curves with increasing draw ratio for the 1/1, 2/1 and 4/1 blends of LMWPE(G808)-UHMWPE. To check the reproducibility of the profile, DSC measurements of films with given draw ratios were carried out several times. Even for undrawn films (λ= 1) with different LMWPE contents, each curve has two peaks. The peaks on low- and high-temperature sides are associated with melting points of LMWPE and UHMWPE crystallites, respectively. The peak position for UHMWPE crystallites slightly shifts to lower temperatures with increasing LMWPE contents. The peak profile at the 1/1 composition is indistinct indicating low crystallinity of LMWPE within the blend film. The peak of LMWPE at the 2/1 composition (67 % LMWPE content) is less intense than that of UHMWPE and a similar tendency was observed even for the 4/1 composition in spite of the 80 % LMWPE content within the blend films. Anyway, the DSC curves indicate that the crystallization of LMWPE and UHMWPE occurred independently by slow evaporation of the solvent under ambient conditions.

On drawing, drastic change in DSC curves was observed. The peak due to LMWPE at 1/1 composition disappears at draw ratios above 20. For the 2/1 composition, the peak disappears at draw ratios above 100, while for the 4/1 composition, a small peak was maintained until the draw ratio reached 200. This is probably due to the co-oriented crystallization of LMWPE and UHMWPE crystallites leading to the growth of crystallites under the preferential orientation process of the c-axis with respect to the stretching direction. Most LMWPE and UHMWPE chains crystallize together to form the same crystallites under crystal transformation by elongation from a folded to a fibrous type. The apparent melting point for all the specimens is lower than the equilibrium melting point (145.5 °C) reported by Flory and Vrij.[16] This phenomenon is quite different from the superheating effect where the melting point observed for UHMWPE films above λ = 100 is higher than 150 °C. This difference will be discussed later.

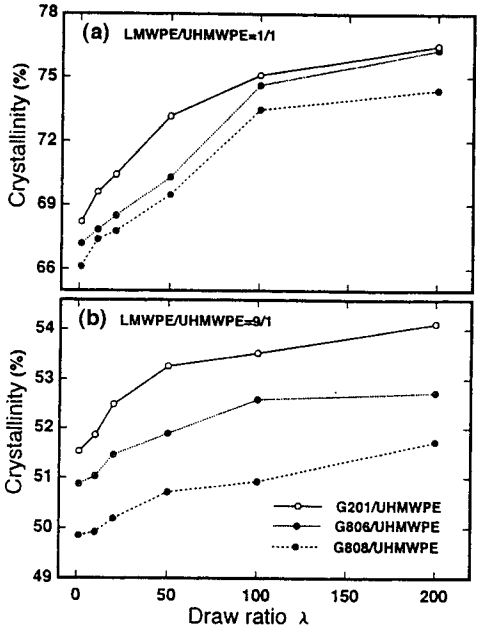

Fig. 5
Change in crystallinity of the LMWPE - UHMWPE blend gel films

Figure 5 shows the change in crystallinity of the LMWPE-UHMWPE blend gel films with increasing draw ratio. The values were estimated from the density, of which parts (a) and (b) correspond to the results for the 1/1 and 9/1 compositions, respectively. The crystallinity increases with the draw ratio. For the 1/1 composition, it is seen that the crystallinities for the three specimens in the undrawn state slightly depend on the molecular weight of LMWPE; the value for the LMWPE(G201)-UHMWPE blend film is the highest. At λ = 200, the crystallinities for the three specimens reached 74-77 %. These values, however, are much lower than the crystallinity (92-94 %) of the UHMWPE gel film at the same draw ratio.[17] This is due to the low crystallinity of branched LMWPE (2.5 CH_3/100 C). For the 9/1 composition, the crystallinities at λ = 1 are lower than those for the 1/1 blends indicating a very low crystallinity of LMWPE in the blend films. This tendency is considerable for the LMWPE(G808) with the shortest chain length. The phenomenon is maintained for the films drawn up to λ = 200. Actually, the crystallinity for the LMWPE(G808)-UHMWPE at λ = 200 is 51.8 % indicating only a 1.9 % increase from 49.9 to 51.8 %. To study this phenomenon, molecular orientational degree was measured by birefringence and X-ray diffraction methods.

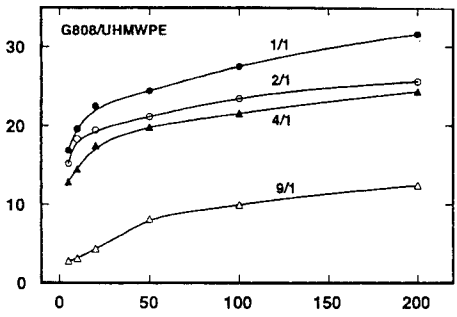

Fig. 6
Change in birefringence of LMWPE(G808) - UHMWPE blend

Figure 6 shows the change in birefringence of LMWPE(G808)-UHMWPE blends with increasing draw ratio. The value at the same draw ratio becomes lower with increasing the LMWPE content. Even the maximum value for the 1/1 blend at λ = 200 is less than 35×10^{-3}, which is much lower than the value (55×10^{-3}) for UHMWPE films. Furthermore, the value for the 9/1 blend at λ = 200 is much lower than that for UHMWPE homopolymer at λ = 20.[18]

This is probably due to the branching effect of LMWPE as discussed before. Anyway, it is evident that the orientational degree of LMWPE chains is less pronounced in comparison with that of UHMWPE chains. In order to obtain more detailed information on molecular orientation, WAXD patterns were obtained.

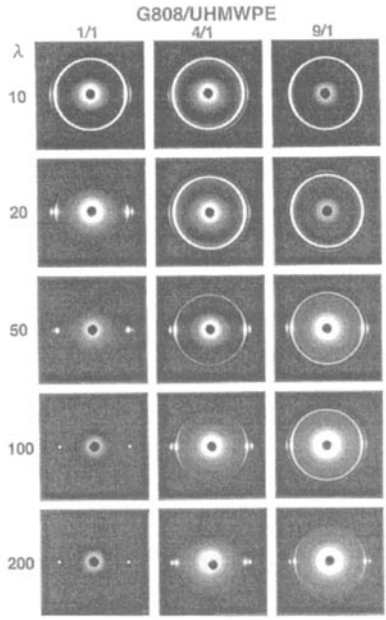

Fig. 7 WAXD patterns from three kinds of LMWPE(G808)-UHMWPE blend films with increasing draw ratio λ

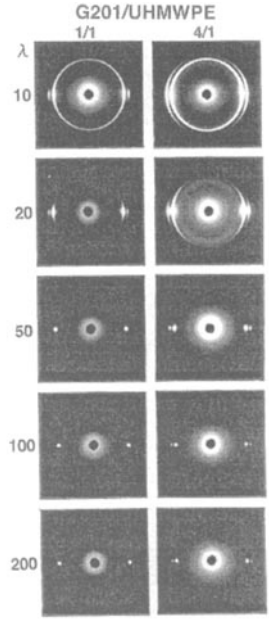

Fig. 8 WAXD patterns from two kinds of LMWPE(G201)-UHMWPE blend films with increasing draw ratio λ

Figure 7 shows the results from three kinds of LMWPE(G808)-UHMWPE blends with increasing draw ratio λ. For 1/1 composition, the sharp reflection spots from the (110) and (200) planes beyond λ = 50 exhibit a high degree of orientation of c-axes with respect to the stretching direction. For 4/1 composition, the pattern shows two kinds of orientational modes for crystallites; one is a high degree of orientation of the c-axes corresponding to the strong equatorial reflection spots and the other is an insufficient orientation corresponding to the large arcs. Sharp spots of the reflection denoting perfect orientation of the c-axis with respect to the stretching direction can be observed for 1/1 composition. The pattern for the 1/1 blend film at λ = 200 shows very small spots from the (110) plane but the reflection of the (200) plane could not be observed indicating preferential orientation of the (200) plane parallel to the film surface. For the 9/1 composition, the patterns also indicate two kinds of orientational modes for crystallites. The large arcs correspond to an insufficient orientation and diffraction rings to random orientation. Although the orientational degree is more pronounced with increasing λ, even at λ = 200, the pattern indicates two kinds of orientational mode of crystallites, a high degree of orientation of the c-axes and an insufficient orientation. This means that large amounts of LMWPE hamper the extremely predominant orientation of the c-axis.

Returning to Fig. 4, it is seen that the DSC curve at λ = 200 shows a single peak at 140 °C for the 1/1 blend, while the curve for the 4/1 blend at λ = 200 shows peaks at 99 and 136 °C. This

indicates that the LMWPE crystallites in the 1/1 blend film become larger by oriented crystallization, while the size of most LMWPE crystallites in the 4/1 blend film is independent of the orientation at $\lambda > 20$. Hence, LMWPE crystallites are assumed to be oriented by accompanying the orientation of UHMWPE crystallites leading to the crystal transformation from a folded to fibrous type; this ensures a suitable level of entanglements between LMWPE and UHMWPE chains which effectively transmit the drawing force.

Figure 8 shows WAXD patterns of two kinds of LMWPE(G201)-UHMWPE blends with increasing draw ratio λ. The orientational behavior of crystallites in the 1/1 blend film is almost the same as that in LMWPE (G808)-UHMWPE blends. In comparison with the patterns for the 1/1 blend, it can be seen that the orientational degree becomes less pronounced as the LMWPE content increases. Even so, the orientational degree at the same composition is higher than that for LMWPE(G808)-UHMWPE blends indicating that a longer molecular chain length even in LMWPE causes a significant effect on the preferential orientation of the c-axis with respect to the stretching direction. Actually, the pattern for the 4/1 blend shows sharp spots at $\lambda = 100$, which is similar to the pattern at $\lambda = 200$ observed for the LMWPE (G808)-UHMWPE blend of 1/1 composition.

In order to study the two orientational modes of crystallites shown in Figs. 7 and 8 in detail, WAXD patterns for LMWPE (G808)-UHMWPE blends, as an example, were observed at elevated temperatures. Figures 9 and 10 show the results for the 4/1 blends at $\lambda = 50$ and 20, respectively, when the sample was fixed at a constant stress of 0.5-5 MPa to avoid the shrinkage of the films. The desirable stress was controlled at each elevated temperature. The specimens were annealed for 10 min at the indicated temperature prior to photographing.

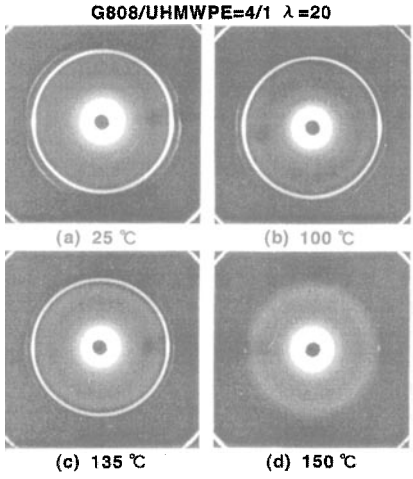

Fig. 9 WAXD patterns of LMWPE(G808)-UHMWPE (4/1) blend films at elevated temperature at $\lambda = 50$

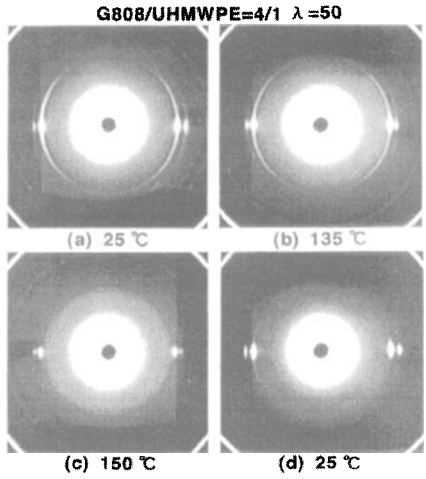

Fig. 10 WAXD patterns of LMWPE(G808)-UHMWPE (4/1) blend films at elevated temperature at $\lambda = 20$

As can be seen in photographs in Fig. 9, the reflections from the (110) and (200) planes slightly shift to smaller diffraction angles. The large arcs disappeared at 150 °C due to melting but the reflection spots remained. Judging from the DSC curves in Fig. 4, it may be concluded that the large arcs are due to the reflection from the LMWPE crystallites with poor preferential orientational degree, while the strong spots are due to the reflection from

UHMWPE crystallites with high orientational degree. As can be seen in Fig.4, the profile of the 4/1 blend film with $\lambda = 50$ shows a small peak around 100 °C and a large peak around 132 °C. These melting points, however, are much lower than those obtained from X-ray diffraction measurements. This discrepancy is due to the difference in heating conditions and in sample setting. In the DSC measurement, heating of the sample was carried out without any constraint through the aluminum sample pan, whereas in the X-ray measurements, the heating was carried out with dimensions fixed in hot air in an oven.

Figure 10 shows the WAXD patterns at $\lambda = 20$ measured at the indicated temperature. The pattern at 25 °C shows a strong diffraction ring from the (110) plane and a weak diffraction ring from the (200) plane. The clear diffraction ring from the (110) plane becomes indistinct with increasing temperature indicating partial melting of crystallites. At 150 °C, the diffraction ring disappeared, indicating the melting of most of crystallites, and diffuse amorphous halo appeared. In spite of the heating temperature beyond the equilibrium melting point (145.5 °C), the specimen could be maintained although the melting point by DSC measurements is much lower than 150 °C. This abnormally high apparent melting point shown in Figs. 9 and 10 may be explained by assuming that polymer chains in the melt state retain the extended-chain arrangement and therefore the entropy of fusion is obviously smaller than the value calculated for random coil in the melt.

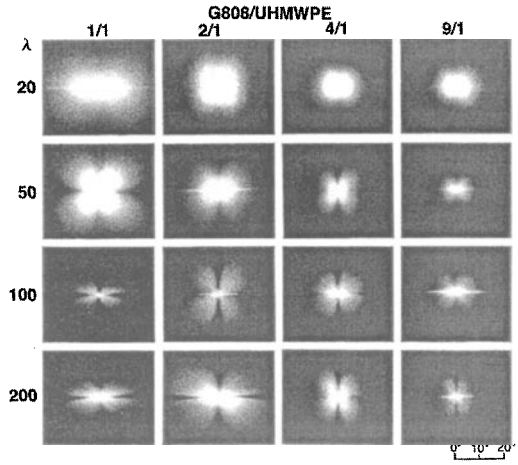

Fig. 11
H_v light scattering patterns from four kinds of blend films of LMWPE(G808)-UHMWPE as a function of the draw ratio

Figure 11 shows H_v light scattering patterns from four kinds of LMWPE(G808)-UHMWPE films (1/1, 2/1, 4/1 and 9/1 compositions) as functions of the draw ratio. Unfortunately, the patterns of undrawn films show circular type because of multiple scattering associated with the film thickness beyond 1 mm. The patterns at $\lambda = 20$ show diffuse lobes somewhat extended in the horizontal direction. Elongation up to $\lambda = 50$ causes development of the X-type pattern and the scattering pattern depending on the LMWPE content.

For the 1/1 blend film, the scattering at $\lambda = 50$ displays four leaf-clover patterns similar to the scattering from spherulitic textures[19] but it is very difficult to discern the positions of the scattering maxima in the lobes. Such a pattern is thought to be due to the two possibilities. One is overlapping scattering from both rod-like[20] and spherulitic textures. The other is the scattering from characteristic textures except for isolated rod-like and spherulitic textures with simple and ideally regular anisotropy. Actually, crystalline superstructure in a film with somewhat low degree of crystallinity has been reported to take a leafstalk texture rather than a spherulitic one. Such characteristic pattern could be realized by theoretical calculations by taking into account the distribution of the spherulite size, taking the spherulite anisotropy

between radial and tangential directions as a function of the distance from the center of the spherulite, making the boundary of the spherulite less clear, and changing the crystalline texture from a spherulitic to a sheaf-like one.[21] On increasing the draw ratio beyond 100, the scattering lobes are extended in the horizontal direction indicating scattering from rods oriented predominantly in the stretching direction. Such patterns are in good agreement with the X-ray diffraction results. In Fig. 7, the WAXD patterns showed very small spots from the (110) plane indicating the perfect orientation of the c-axis with respect to the stretching direction. If this is the case, the disappearance of light scattering patterns must be discerned because of the disappearance of the rod-like texture due to the transformation into a fibrous structure. Actually, the pattern from UHMWPE homopolymer with $\lambda = 200$ showed sharp streaks due to the scattering from sharp cracks and fine filaments appearing by the disruption of rods.[7] Nevertheless, the pattern of the 1/1 blend indicates the scattering from oriented rods composed of LMWPE crystallites with folded structure. This remains an unresolved problem.

For blends with the 2/1, 4/1 and 9/1 compositions, the patterns are sensitive to the LMWPE content. Elongation beyond $\lambda = 50$ gives a distinct X-type pattern with azimuthal angle dependence. A close observation reveals that the lobes of the blend film with the 4/1 composition change from the horizontal to meridional direction at $\lambda > 50$ but the lobes for the 9/1 composition are extended in the horizontal direction up to $\lambda = 100$ and further elongation gives a profile change from the horizontal to the meridional direction. Considering the theory of small-angle H_v light scattering, such lobes extended in the meridional direction must be interpreted as a contribution of scattering from rods, with extremely high orientation perpendicular to the stretching direction. This phenomenon was already confirmed to be due to oriented crystallization during elongation.[22,23] The corresponding X-ray patterns in Fig. 7 show very sharp spots with strong intensity due to the reflection from UHMWPE, and diffraction ring or very long arcs due to the reflection from LMWPE. The WAXD and H_v light scattering patterns together indicate that the blend films composed of rods constructed from LMWPE and the change in the profiles under elongation reflect the orientational behavior of the rods with a folded structure which were maintained without disruption.

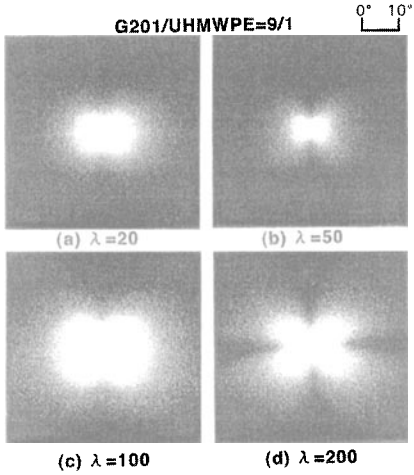

Fig. 12 H_v light scattering patterns from LMWPE(G201)-UHMWPE blend films with 9/1 composition as a function of the draw ratio

Figure 12 shows H_v light scattering patterns from the 9/1 blend of LMWPE(G201)-UHMWPE system as a function of the draw ratio. The lobes are extended to the horizontal direction with increasing λ, which are essentially similar to those obtained for 1/1 blends of LMWPE(G808)-UHMWPE. According to the previous result for LMWPE(G201)-UHMWPE films with LMWPE content $\leq$ 50 %,[15] the patterns up to $\lambda = 200$ were dependent on the LMWPE/UHMWPE composition. For the blends with LMWPE content < 35 %, the pattern indicated the existence of rod-like texture since the intensity had a maximum in the scattering center decreasing monotonically with increasing scattering angle. In contrast, the notch of the lobes for the 1/1 blend (50 % LMWPE content) is clear, especially in the scattering center region. However, the observation of the scattering maxima in the lobes was very difficult, indicating overlapping scattering from both rod-like and spherulitic

textures. In the present case, however, the patterns from the 9/1 blend film as shown in Fig. 12 are quite different from the previous results observed for the blend films with LMWPE content ≤ 50 %.[15] The present patterns are mainly due to scattering from rods, which were constructed by LMWPE. As shown in Fig. 12, the patterns at λ ≤ 100 show indistinct profile but the elongation up to λ = 200 causes development of a clear X-type pattern whose lobes are extended in the horizontal direction indicating the oriented rods with clear optical anisotropy parallel to the stretching direction. This phenomenon associated with oriented crystallization under elongation is similar to that observed for LMWPE (G808)-UHMWPE blend with 1/1 composition.

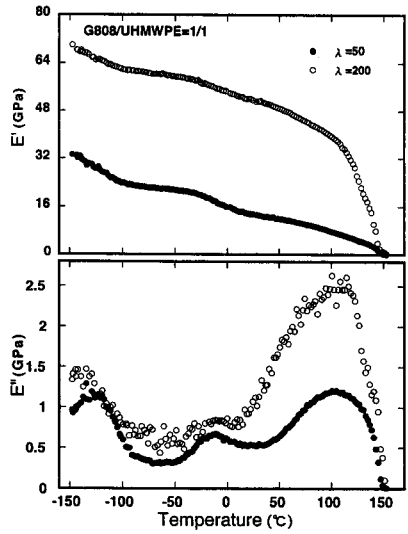

Fig. 13 Temperature dependence of the storage and loss moduli for 1:1 with LMWPE(G808)-UHMWPE blend films with λ = 50 and 200

Figure 13 shows the temperature dependence of the storage and loss moduli for the blend films with LMWPE(G808)/UHMWPE = 1/1 which were drawn to λ = 50 and 200. The storage modulus becomes higher with λ because of the increase in crystallinity and molecular orientation shown in Figs. 4 and 7. The storage modulus at 20 °C at λ = 200 reached 53 GPa but the value is about one third of the value obtained for UHMWPE homopolymer films.[17]

The loss modulus has three peaks. A peak around 100 °C corresponds to the crystal dispersion (the α mechanism) associated with grain boundary phenomena due to the rotation of crystal grains, as well as associated with the smearing-out effect of the crystal lattice potential due to the onset of rotational oscillation of polymer chains within the crystal grains.[24] The magnitude becomes pronounced with increasing λ. A peak of the β mechanism can be observed clearly around –10 °C because of the branching of LMWPE (2.5 CH_3/100 C). Incidentally, the β peak has never been clearly observed for UHMWPE films with λ > 50 because of high crystallinity (> 90 %). The crystallinities of blend films with the 1/1 composition are about 70 % at λ = 50 and about 74 % at λ = 200 . The appearance of the β peak is attributed to the molecular chain motions in amorphous phase.[25] In comparison with the two results in Figs. 13 and 5, it may be expected that the higher the amorphous fraction, the more intense the β peak is. The dispersion peak termed the γ mechanism appeared at -120 to -130 °C, which has been reported as the local motions of side groups in the amorphous region and/or defects in the crystalline phase.[24] The magnitude is confirmed to be almost the same as that of UHMWPE films at the corresponding draw ratio.

Figures 14-16 show the temperature dependence of the storage and loss moduli for the three kinds of blend films with the indicated compositions at λ = 200. The storage modulus in the given temperature range decreased drastically with increasing LMWPE contents. The storage modulus of LMWPE (G808)-UHMWPE is lower than that of LMWPE(G201)-UHMWPE and that of LMWPE (G806)-UHMWPE. This is probably due to the fact that chain length of LMWPE (G808) is the shortest and, consequently, the number of entanglements between LMWPE (G808) and UHMWPE chains is the lowest. This tendency becomes considerable with increasing LMWPE content. For example, the values of LMWPE (G808)-UHMWPE blend films with the 4/1 and 9/1 compositions at 20 °C are 12 and 8 GPa, respectively,

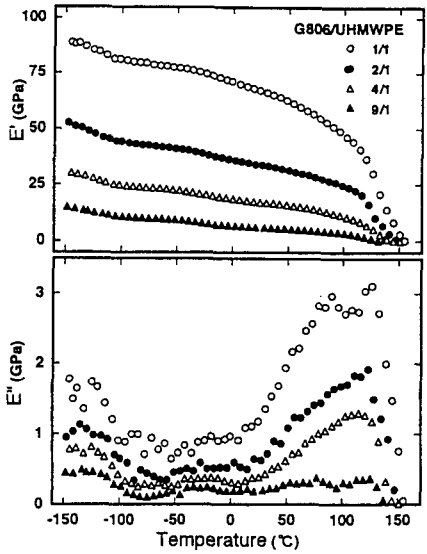

Fig. 14 Temperature dependence of the storage and loss moduli of LMWPE(G808) -UHMWPE blend films with the indicated compositions at $\lambda = 200$

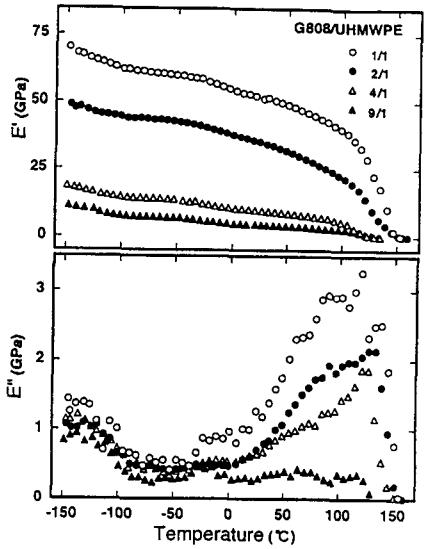

Fig. 15 Temperature dependence of the storage and loss moduli of LMWPE(G806) -UHMWPE blend films with the indicated compositions at $\lambda = 200$

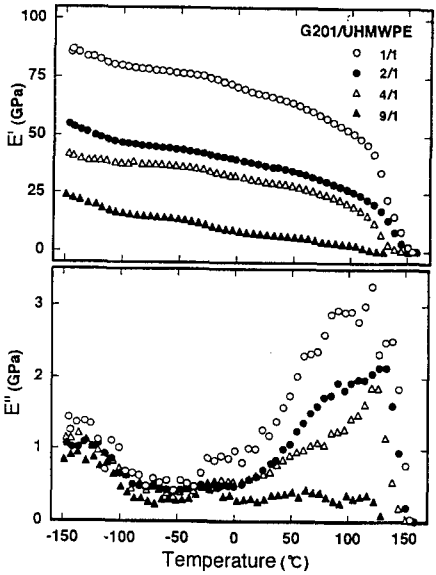

Fig. 16
Temperature dependence of the storage and loss moduli of LMWPE(G201)-UHMWPE blend films with the indicated compositions at $\lambda = 200$

which are almost equal to that observed for melt films drawn 8 - 10 fold. In spite of a very small value of the storage modulus, the WAXD pattern of the 4/1 blend with $\lambda = 200$ shows very strong small spots indicating the extremely high orientation of the c-axis as discussed before (see Fig. 7). The draw ratio of UHMWPE films which gives the diffraction spots of the same size was about 50 and the corresponding Young's (storage) modulus was 25 - 30 GPa. This means that the high-modulus material cannot be prepared by introducing large amounts of LMWPE even if the molecular orientation is almost perfect. This is probably due to the

fact that the number of entanglements is too low to effectively transmit the drawing force to affect the LMWPE crystal transformation from a folded to a fibrous type. For the 9/1 blend film with $\lambda = 200$, this characteristic property became clearer. The WAXD pattern shows two orientational modes with a very high degree of orientation of the c-axis and an insufficient orientation (Fig. 7). Even so, the total orientation of c-axis takes a high degree of orientation. However, as discussed before, Young's modulus is about 8 GPa. This supports the assumption that the low Young's modulus is also attributed to few entanglements. Here we must emphasize that LMWPE cannot form dry gel films but the introduction of a small amount of UHMWPE surely plays an important role in forming dry gel films with significant drawability (up to $\lambda = 200$). Unfortunately, Young's modulus is less than 10 GPa. Through the series of experimental results, it may be concluded that the LMWPE content in the blend films must be lower than 50 % to produce high-modulus and high-strength materials.

Conclusion

Ultrahigh-molecular-weight polyethylene (UHMWPE) and low-molecular-weight polyethylene (LMWPE) blend films were prepared by gelation/crystallization from solutions. The viscosity-average molecular weight ($\overline{M}_v$) of UHMWPE was 6×10^6, while three kinds of LMWPE with $\overline{M}_v = 4.13\times10^4$, 1.95×10^3 and 1.53×10^3 were used. The LMWPE/UHMWPE compositions were 1/1, 2/1, 4/1 and 9/1. Gels with 9/1 composition (90% LMWPE content) could form a film by evaporating the solvent, although LMWPE homopolymer gels are not able to form a film. The resulting films with the above compositions could be readily elongated in a hot oven up to 200-fold. Such high elongation is assumed to be due to the existence of a suitable level of entanglements between LMWPE and UHMWPE chains.

The orientational mode of crystallites was sensitive to the composition even at the same draw ratio. Although the orientational degree of LMWPE crystallites became poorer as the LMWPE content increases, LMWPE crystallites within the 1/1 blend film took extremely high orientation like the UHMWPE homopolymer. In contrast, the orientational degree of LMWPE crystallites for the 4/1 blend film was much less pronounced in comparison with that of UHMWPE crystallites. Such orientational behavior was related to a suitable number of entanglement meshes. The poor orientation of LMWPE crystallites with increasing LMWPE content was attributed to the decrease in the number of entanglements between LMWPE and UHMWPE chains. In this case, the orientational mode of LMWPE crystallites under elongation is assumed to be due to the preferential orientation of the c-axis with respect to the stretching direction, mainly by crystal rotation leading to strained tie molecules.

DSC curves of the undrawn films show two peaks corresponding to the individual homopolymers indicating that crystallization of LMWPE and UHMWPE occurred independently by evaporation of the solvent under ambient conditions. When the blend film with the 1/1 blend was stretched, the peak due to LMWPE crystallites disappeared above $\lambda = 20$. This means the co-oriented crystallization of LMWPE and UHMWPE crystallites under elongation leading to crystal transformation from a folded to fibrous type. For the other compositions, two peaks were maintained. In this case, the orientation of UHMWPE crystallites is related to the crystal transformation, while that of LMWPE to rotation of crystallites.

The storage modulus of the blend films at the same draw ratio decreased as the LMWPE content increased. The storage modulus of the 1/1 blend film with $\lambda = 200$ remained about 60 GPa at 20 °C and this value is sufficient for usual applications of polyethylene fibers. However, the storage modulus decreased drastically with increasing the LMWPE content. For the 9/1 blend film, the modulus is less than 10 GPa at 20 °C, which is lower than that of melt-spinning fibers of LMWPE.

References

1) Smith, P.; Lemstra, P.J.; Kalb, B.; Pennings, A. *Polym. Bull.* (1979) **1** 733
2) Smith, P.; Lemstra, P.J. *J. Mater. Sci.* (1980) **15** 505
3) Smith, P.; Lemstra, P.J.; Booij, H.C. *J. Polym. Sci., Polym. Phys. Ed.* (1981) **19** 877
4) Smith, P.; Lemstra, P.J.; Pippers, J.P.L.; Kiel, A.M. *Colloid Polym. Sci.* (1981) **258** 1070
5) Ogita, T.; Yamamoto, R.; Suzuki, N.; Ozaki, F.; Matsuo, M. *Polymer* (1991) **32** 822
6) Matsuo, M.; sawatari, C.; Iida, M.; Yoneda, M. *Polym. J.* (1985) **17** 1197
7) Matsuo, M.; Inoue, K.; Abuymiya, N. *Sen-i-Gakkaishi* (1984) **40**, 275
8) Matsuo, M.; Manley, R.St.J. *Macromolecules* (1982) **15** 985
9) Matsuo, M.; Manley, R.St.J. *Macromolecules* (1983) **16** 1505
10) Sawatari, C.; Okumura, T. Matsuo, M. *Polym. J.* (1986) **18** 741
11) Kang,S.J.; Matsuo, M. *Polym. J.* (1988) **21** 49
12) Bunn, C.W. *Trans. Faraday Soc.* (1939) **35** 482
13) Matsuo, M.; Sawatari, C.; Ohhata, T. *Macromolecules* (1988) **21** 1317
14) Sawatari, C.; Matsuo, M. *Macromolecules* (1987) **20** 1033
15) Sawatari, C.; Matsuo, M. *Polymer* (1989) **30** 1603
16) Flory , P.J.; Vrij, A.J. *J. Am. Chem. Soc.* (1963) **85** 3548
17) Matsuo, M.; Sawatari, C. *Macromolecules* (1986) **19** 2036
18) Sawatari, C.; Matsuo, M. *Macromolecules* (1986) **19** 2726
19) Stein, R.S.; Rhodes, M.B. *J. Appl. Phys.* (1960) **31** 1873
20) Rhodes, M.B.; Stein, R.S. *J. Polym. Sci. Part A-2* (1969) **7** 1539
21) Motegi, M.; Oda, T.; Moritani, M.; Kawai, H. *Polym. J.* (1970) **1** 209
22) Sawatari, C.; Iida, M.; Matsuo, M. *Macromolecules* (1984) **17** 1765
23) Sawatari, C.; Yamamoto, Y.; Yanagida, N.; Matsuo, M. *Polymer* (1993) **34** 956
24) Kawai, H.; Suehiro, S.; Kyu, T.; Shimomura, A. *Polym. Eng. Rev.* (1983) **3** 109
25) Hoffmann, J.D.; Williams, G.; Passaglia, E. *J. Polym. Sci. C* (1966) **14** 173